Mutants of the Membrane-binding Region of Semliki Forest Virus E2 Protein.
I. Cell Surface Transport and Fusogenic Activity

Daniel F. Cutler and Henrik Garoff

European Molecular Biology Laboratory, 6900 Heidelberg, Federal Republic of Germany. Dr. Cutler's present address is Department of Biochemistry and Biophysics, University of California, San Francisco, School of Medicine, San Francisco, California 94143.

Abstract. Three mutations of the membrane-binding region of the Semliki Forest virus (SFV) p62 polypeptide (the precursor for virion E3 and E2) have been made by oligonucleotide-directed mutagenesis of a cDNA clone encoding the SFV structural proteins. One of the mutations (A2) substitutes a Glu for an Ala in the middle of the hydrophobic stretch which spans the bilayer. A1 and A3 alter the two basic charged amino acids in the cytoplasmic domain next to the hydrophobic region. The wild-type charge cluster of Arg-Ser-Lys (+2) has been changed to Gly-Ser-Met (0;A3) or to Gly-Ser-Glu (−1;A1). The mutant p62 proteins have been analyzed both in the presence and the absence of E1, the other half of the heterodimer spike complex of SFV. The mutant proteins expressed in COS-7 cells are glycosylated and are of the expected sizes. When co-expressed with E1, all three mutants are cleaved to yield the E2 protein and transported to the surface of COS-7 cells. When expressed in the absence of E1, the mutant p62 proteins remain uncleaved but still reach the cell surface. Once at the cell surface, all three mutants, when co-expressed with E1, can promote low pH–triggered cell–cell fusion. These results show that the three mutant p62/E2 proteins are still membrane associated in a functionally unaltered way.

TRANSMEMBRANE proteins that span the lipid bilayer once can be divided into three protein domains: lumenal (or external), transmembrane (or hydrophobic), and cytoplasmic. Some of these proteins have been shown to be oriented in the membrane with their COOH-terminus in the cytoplasm (group I membrane proteins; see reference 16) while others have the opposite orientation (group II). We are attempting to define the features of group I transmembrane proteins that lead to the establishment and maintenance of their three-domain structure.

A large number of biochemical and structural studies (e.g., 8, 13, 23, 42, 47, 49, 51) on group I proteins have demonstrated that the transmembrane protein domain consists of a long stretch (20–30) of hydrophobic and neutral amino acid residues. In addition, sequence comparisons between group I proteins have revealed that the hydrophobic peptide is always followed by one or more positively charged residues (the "charge cluster") immediately preceding the cytoplasmic domain. These basic residues have also been implicated in membrane binding, e.g., by interacting with negatively charged phospholipid headgroups on the cytoplasmic membrane surface (47, 51). The observation that the transmembrane peptide and the charge cluster of group I proteins are generally encoded by one single exon (e.g. 20, 34) supports the notion that the two consensus features are functionally related. Our working hypothesis is that the region containing the hydrophobic transmembrane domain and the charge cluster of the cytoplasmic domain make up the membrane-binding region of group I proteins.

It has been postulated that the generation of the three-domain structure of group I proteins occurs co-translationally. Group I proteins have been shown to be inserted across the endoplasmic reticulum membrane starting from their NH_2-termini using the same mechanism as secretory proteins (see, e.g., 25, 26, and 33). However, in contrast to secretory proteins, where chain transfer is completed, translocation of a membrane protein chain is thought to be arrested at the level of its hydrophobic segment by a "stop transfer signal," thus resulting in a transmembrane protein (4; for review see reference 47). A most likely candidate for this "stop transfer signal" could be the membrane-binding region of group I proteins. Such a role for this region is supported by a great deal of evidence derived both from natural variants of certain proteins and more recently from studies with mutations engineered in vitro. The evidence may be arranged into several categories. Firstly, loss of both hydrophobic domain and cytoplasmic tail, as would be predicted, leads to secretion from the cell (IgG, IgM, IgA, and IgD [e.g., 2, 44], Herpes envelope protein [24], and H-2 related pH 16 [30] are natural variants; influenza hemagglutinin [17], and Vesicular Sto-

matis virus glycoprotein [VSV-G][1] [45] are derived from deliberate engineering). Alternatively, the truncated proteins are still cell associated but no longer transmembrane proteins (one mutant of the low density lipoprotein receptor provides a natural example [32]; phage F1 gene III protein [5] and Rous Sarcoma virus envelope protein [53] are engineered examples). These data do not exclude the possibility that the cytoplasmic tail could be involved in anchoring. However, there are examples of proteins in which the normal cytoplasmic tail alone has been partially or completely (with the exception of the charge cluster) removed, and membrane association is apparently not affected. H-2 antigens (56), VSV-G (46), influenza hemagglutinin (12), Semliki Forest virus (SFV) E2 (15), and Rous Sarcoma virus envelope protein (53) have all been investigated in this respect. To demonstrate that the functioning of the hydrophobic domain is also independent of the lumenal domain, the lumenal domains of several group I proteins have been exchanged generating fusion proteins that are still membrane associated (F1 gene III protein/gene VIII protein [5], SFV-E2/VSV-G [43], SFV-E2/Fowl Plague virus–hemagglutinin [43], growth hormone/VSV-G [19], and influenza hemagglutinin/VSV-G [38]). Finally, and most elegantly, Yost et al. (54) placed the membrane-binding polypeptide region of an IgM heavy chain between the bacterial β-lactamase (NH$_2$-terminal) and chimpanzee α-globin (COOH-terminal). This chimera had the topology predicted by the stop transfer postulate.

We decided to study the features of the membrane-binding region of a group I polypeptide that are important for its function using the extremely powerful approach of in vitro mutagenesis followed by in vivo expression. The model protein we are using is the well-characterized group I protein p62/E2 of SFV (14, 48) (see also Figs. 1 and 4). The p62 protein is a 486–amino acid residues–long transmembrane spike glycoprotein which is synthesized in the rough endoplasmic reticulum and then transported as a complex with the other SFV spike glycoprotein E1 to the cell surface. At the plasma membrane, the p62 protein is cleaved after residue 66 to form E3 and E2. The p62/E2 protein has a 31-residue COOH-terminal cytoplasmic tail with a "typical" charge cluster (Arg-Ser-Lys) flanking the transmembrane domain. Using oligonucleotide-directed mutagenesis, three mutants have been produced in the membrane-binding region: A1, changing the positive charge cluster from Arg-Ser-Lys (+2) to Gly-Ser-Glu (−1); A2, substitution of the negatively charged Glu for an Ala in the middle of the uncharged hydrophobic spanning region; A3, changing the charge cluster from wild type (+2) to Gly-Ser-Met (0).

The phenotypes of the p62/E2 mutants will depend on the function of the altered regions in translocation arrest and membrane binding. It was originally proposed (4) that a "stop transfer" signal was recognized by some element of the translocation machinery, causing the disassembly of a proteinaceous tunnel in the membrane through which secretory and membrane proteins are translocated, thereby trapping a membrane protein in the bilayer. According to this model, the mutants might no longer have functional signals and the

tunnel might then remain in place. The proteins would then complete translocation becoming lumenal proteins, either cell associated or secreted. On the other hand, if the membrane-binding region interacts either directly with the lipid bilayer, or is recognized in a degenerate fashion by the translocation machinery, then the mutations may have more subtle effects on membrane binding and/or topology. The mutant phenotypes would then reflect the relative roles of the two features of this region in establishment and maintenance of topology.

In this paper, we show that all three mutants are still membrane associated in a functionally unaltered fashion since they are all capable of reaching the cell surface where they can promote normal low pH–triggered cell–cell fusion. In the accompanying paper we assay the topology and membrane-binding capacity of the SFV-A mutants directly.

Materials and Methods

General DNA Manipulations

Except where stated, all enzymes were from Boehringer Mannheim Biochemicals, Indianapolis, IN or New England Biolabs, Beverly, MA. General molecular biological techniques were performed as described (35). Transformation of *Escherichia coli* (except where otherwise stated, strain 71/18 [40]) was performed as in Hanahan (21). Preparation of DNA was as described (27).

Vectors

To construct pSFd, the origin of replication of the phage F1 was isolated from pD4 (11) as an EcoRI fragment, and the ends were filled in and then ligated into pS-S-SFV at the PvuII site. One of the two EcoRI sites was recreated (see Fig. 2a).

Wild-type pS-S-SFV has been described elsewhere (27). pL1-SFV was obtained by isolating the Hind III–Hind III fragment which codes for the SFV structural proteins from pS-S-SFV, filling in the ends, adding Bam HI linkers, and cloning it into the unique BamHI site of pA11-SVL2 (18).

pL1-SFV-d9 was derived from pSV2-SFV-d9 (one of the series of the SFV deletion mutations described by Garoff et al. [15]). The deletion mutant d9 encodes capsid and p62 but not E1. In d9, the truncated 6K is followed by eight aberrant amino acids introduced by the stop translation linker (Garoff, H., unpublished data). pL1-SFV-d9 was produced by a three-fragment ligation. Fragments were prepared as follows. (a) pSV2-SFV-d9 was linearized with Hind III, the ends filled in and BamHI linkers added. This was then cleaved with ClaI and the ClaI–BamHI fragment containing the SFV coding region was isolated. (b) pkTH601 (41) was cut with BamHI and Cla I and the small fragment containing the translation stop linker was isolated. (c) pA11-SVL2 was cut with BamHI and treated with phosphatase. All three isolated fragments were then ligated together, and colonies resulting from transformation screened for pL1-SFV-d9 by restriction analysis.

Mutagenesis

Oligonucleotides were purchased from Dr. Kaplan, City of Hope, Research Institute, Duarte, CA.

Mutagenesis of SFV-A1 and A2. Following the procedures of Dente et al. (10), single-stranded DNA (ssDNA) was prepared from pSFd. The conversion of this material to double-stranded (ds) pSFd incorporating the mutagenic oligonucleotide in vitro was as described in Zoller and Smith (55) using Klenow (Bethesda Research Laboratories, Gaithersburg, MD) and T4-DNA ligase (kind gift of F. Winkler, Hoffman–LaRoche, Basel, Switzerland). The heteroduplex was cut with SstII, the small fragment isolated and ligated into the large fragment isolated from SstII-digested, phosphatase-treated pS-S-SFV. This ligation was used to transform *E. coli* and resultant colonies were screened for mutants by hybridization to the mutagenic oligonucleotide as described in Carter et al. (7). The putative mutants of pS-S-SFV were digested with PvuII and ScaI, and the ends were filled in. The small fragment isolated and ligated into M13 mp8 (39, 40) that had been cut with SmaI and phosphatased (see Fig. 2b). M13 mp8-SFV was then used for confirmatory sequencing between the SstII sites using the dideoxy chain–terminating method. The mutant pS-S-SFVs were then used for expression or used for subcloning the mutants into pL1-SFV and pL1-SFV-d9.

Mutagenesis of SFV-A3. M13 mp8-SFV was generated from wild-type pS-S-SFV as described above. M13 mp18 was digested with EcoRl and Hind III. The large fragment was isolated and 2 pmol incubated in 16 μl of buffer A (25 mM Tris, pH 7.5, 60 mM NaCl, 12.5 mM MgCl₂, 2 mM dithiothreitol) at 95°C for 10 min. 0.5 pmol (1 μl) of ssM13 mp8-SFV was added and the material transferred to 65°C for 1 h, followed by addition of 30 pmol (3 μl) of kinased oligonucleotide. The mixture was then slowly cooled to room temperature. 18 μl of buffer C (buffer A + 1 mM of each dNTP + 1 mM ATP) followed by 1 U DNA ligase and 2.5 U DNA polymerase 1 (large fragment) were added, and incubated for 3 h at 16°C. Aliquots were used to transform ES871 (6), and hybridization screening was carried out as for SFV-A1/A2. Confirmatory sequencing between Sst-II sites was carried out by the dideoxy method in m13 mp18-S-SFV and the SstII–SstII fragment was subcloned into the various expression vectors.

DEAE–Dextran-mediated Transfection of COS-7 Cells

Subconfluent monolayers of COS-7 cells (~2 × 10⁶ cells) on 5-cm dishes were transfected as follows. Plasmid DNA was diluted in RPMI 1640 (Gibco, Grand Island, NY) to 4 μg/ml and mixed with an equal volume of DEAE–dextran (Pharmacia Fine Chemicals, Piscataway, NJ; molecular weight, 5 × 10⁵) in RPMI 1640 at a concentration of 2 mg/ml. Cells were washed twice with RPMI and then incubated with the DNA mix (1 ml/dish). After 1 h at room temperature, 5 ml of Dulbecco's modified Eagle's medium (DME) with 10% fetal calf serum and 10% dimethyl sulfoxide were added. 3 min later, the cells were washed twice with DME plus 10% fetal calf serum supplemented with 40 μM chloroquine (Sigma Chemical Co., St. Louis, MO) and left in this solution for 6 h at 37°C. The cells were then washed and incubated for 30 or 40 h at 37°C in 5 ml DME plus 10% fetal calf serum before labeling, fixation, or lysis.

Microinjection, Immunofluorescence, Western Blotting, and Gel Electrophoresis

Microinjection and indirect immunofluorescence were performed as described (50). Western blotting was performed as described in Kondor-Koch et al. (27). Quantitation of Western blots was performed as follows: ¹²⁵I-protein A (New England Nuclear, Boston, MA) was used as a second antibody instead of peroxidase-conjugated sheep anti-rabbit IgG (Biosys, Compiegne, France). The blot was rinsed, air dried, and exposed to X-ray film between screens (Cronex double-lightning; DuPont Co., Wilmington, DE). Autoradiographs were scanned on a Helena Laboratories Quick Scan densitometer (Desaga, Heidelberg, Federal Republic of Germany), and peaks were cut out and weighed.

Fusion Assay

The assay for cell–cell fusion after microinjection of BHK-21 cells has been described (27).

Biosynthetic Labeling and Use of Tunicamycin

Cells were labeled 30 h after transfection with [³⁵S]methionine (800 Ci/mmol; Amersham Corp., Arlington Heights, IL) at 1 mCi/5-cm dish. The cells were washed twice with DME minus methionine, starved for 15 min, and then incubated in DME minus methionine plus the [³⁵S]methionine for 1 h. To study glycosylation, cells were incubated in 4 μM tunicamycin (Calbiochem-Behring Corp., La Jolla, CA) for 2.5 h, labeled for 1 h (in the presence of tunicamycin), and then lysed.

Immunoprecipitation

5-cm dishes of transfected cells were placed on ice and washed twice with ice-cold phosphate-buffered saline. This was replaced with 500 μl of lysis buffer (1% Nonidet P-40, 150 mM NaCl, 50 mM Tris, pH 7.5) supplemented with a range of protease inhibitors (phenylmethylsulfonyl fluoride, leupeptin, trasylol, pepstatin, benzamidine, and antipain [all from Sigma Chemical Co.], used as described in reference 37). After 5 min on ice, the cell lysate was removed and spun for 2 min in a microfuge to remove nuclei and other insoluble material. For immunoprecipitation, the volume and composition of the buffer were then adjusted to 1% Nonidet P-40, 1% deoxycholate, 0.1% SDS, 150 mM NaCl, 50 mM Tris, pH 7.6, in 1 ml. 50 μl of Pansorbin (Calbiochem-Behring Corp.) washed in lysis buffer was added and the lysate rocked at room temperature for 30 min. After centrifugation at 100,000 g for 1 h at 4°C, the supernatant was incubated overnight at 4°C with 1 μl rabbit anti-E2 IgG or 10 μl of an affinity-purified fraction prepared from this. 50 μl of Pansorbin was added, and the mixture rocked at room temperature for 30 min. The Pansorbin was then repeatedly washed and pelleted in a microfuge with the following buffers: lysis buffer plus 5 mM EDTA (twice); lysis buffer plus EDTA plus 350 mM NaCl (once); and 10 mM Tris, pH 7.5 (twice). The final pellet was resuspended in 50 μl of sample buffer (200 mM Tris, pH 8.8, 1.0 M sucrose, 0.01% bromophenol blue, 5 mM EDTA, 4% SDS), reduced with dithiothreitol, heated to 95°C for 5 min, and alkylated with iodoacetamide.

Results

### Construction of the SFV-A Mutants

The three mutants of the membrane-binding polypeptide region (Fig. 1) of p62/E2 have been constructed using oligonucleotide-directed mutagenesis (55). Briefly, the procedure begins with generating an ssDNA copy of the region to be mutated. An oligonucleotide containing the desired alterations plus wild-type overlaps at each end is hybridized to the ssDNA template and used as a primer for DNA polymerase I to convert this material back to dsDNA in vitro. The in vitro-synthesized heteroduplex is then replicated in vivo and daughter plasmids containing the mutation are isolated. The mu-
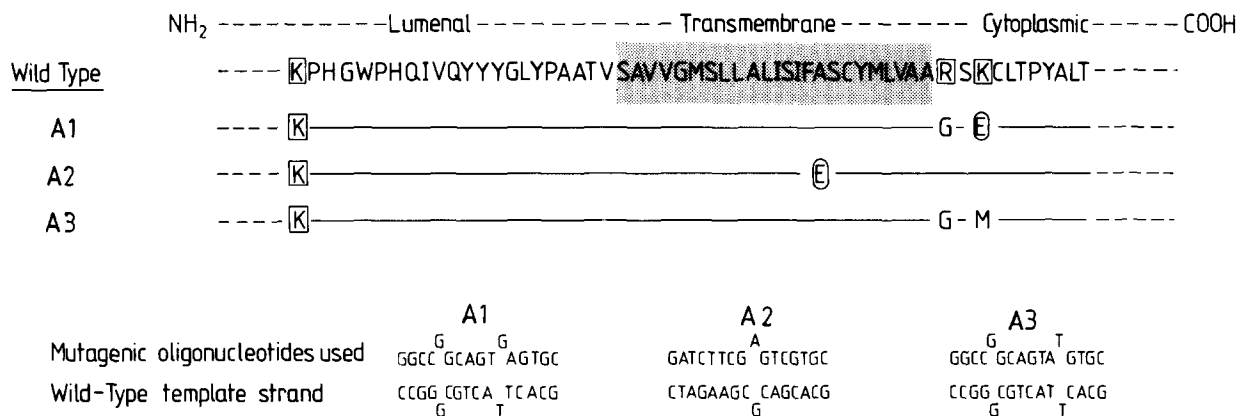
Figure 1. Predicted primary structures of the SFV-A mutants. This schematic diagram, using the single-letter code of the amino acid sequence around the membrane-spanning region, includes the following features: basic amino acids are boxed, acidic are encircled. The shaded region of the wild type indicates the probable membrane-spanning region. The amino acids indicated in the mutants are those changed from wild type. The mutagenic oligonucleotides used to make the changes are shown, along with the corresponding region of template. The oligonucleotides are shown 5′ to 3′ left to right. The mismatches are indicated by raising (in the mutagen) and lowering (in the template) the relevant bases.

Figure 2. Flow diagrams (not to scale) of the construction of the SFV-A mutants. *A* (*left page*) shows the steps involved in the construction of SFV-A1 and SFV-A2. *B* (*right page*) shows the steps involved in the construction of SFV-A3. Two concentric circles indicate dsDNA, a single circle indicates ssDNA. In pSFd (*A*), the SFV transcript is indicated in the outer semicircle with boxed coding region. Functional regions of the plasmids pSFd and pS-S-SFV in *A* are indicated: solid (black) color, SFV cDNA; hatching, SV40 early promoter; cross-hatching, polyadenylation signals for SV40; stippling, F1 origin of replication; unshaded, pBR322 ampicillin resistance and origin of replication. Arrowheads within plasmids indicate the action of DNA polymerase.
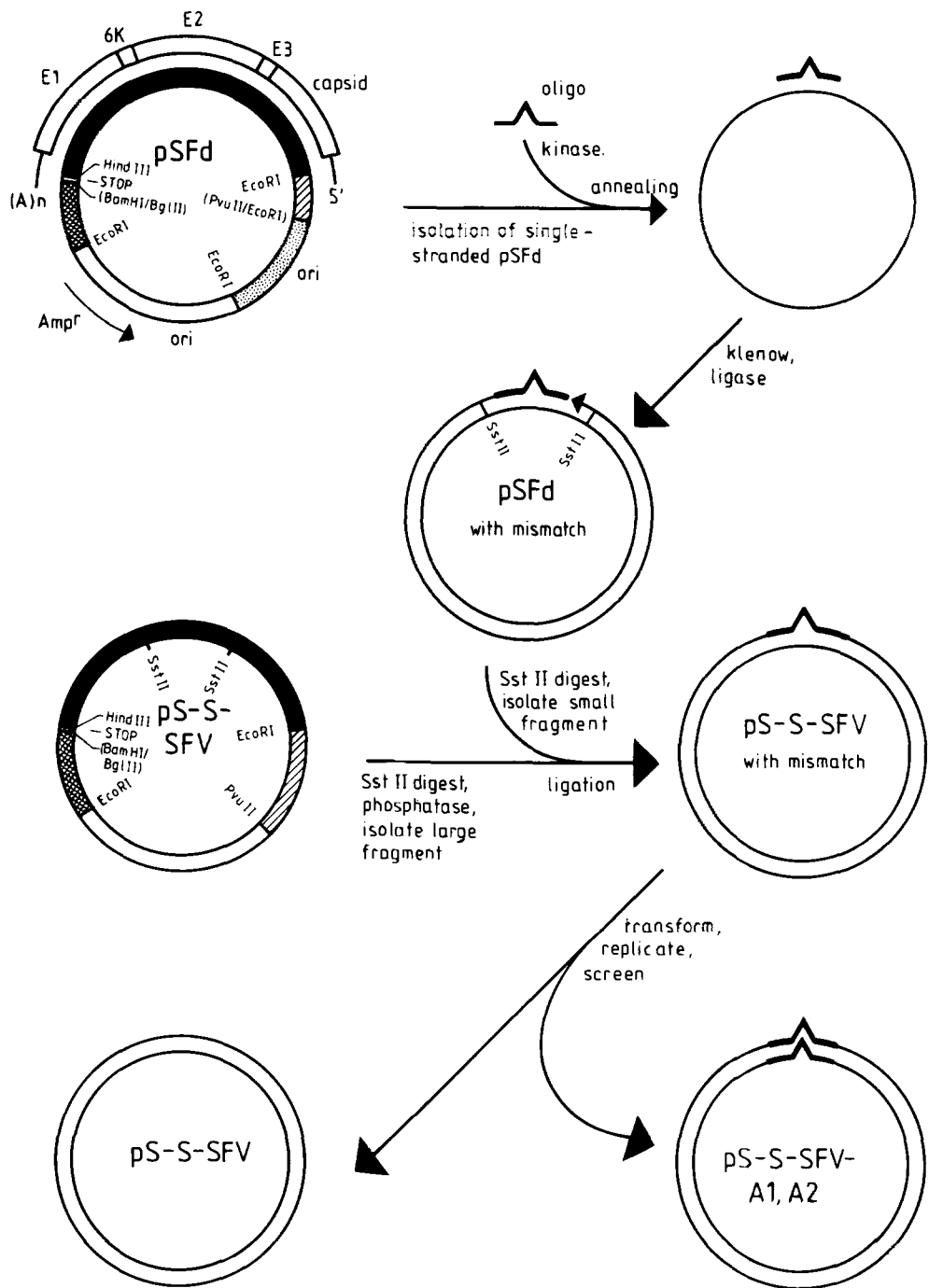
tagenic oligonucleotides and complementary template regions used to create the SFV-A mutants are shown (with mismatches) in Fig. 1. The oligonucleotides were designed both to make the desired amino acid changes and to introduce new restriction sites into the DNA to facilitate screening for mutated plasmids. A1 and A3 introduce HpaII sites (CCGG), whereas A2 introduces a TaqI site (TCGA).

The strategies used for mutagenesis (Fig. 2, *a* and *b*) were designed to minimize undesired mutations caused by the oligonucleotide hybridizing to secondary sites on the template ssDNA, resulting in false positives during screening. Because the SFV cDNA is 3,983 base pairs long (14), many such sites existed, and were used by the mutagenic oligonucleotides (Cutler, D., unpublished observations). Thus, for SFV-A1 and SFV-A2 (Fig. 2*a*), the region of mutagenized DNA that was screened was limited to a 149-base pair SstII–SstII fragment transferred to a wild-type vector. The ssDNA template for SFV-A1 and SFV-A2 was produced using the approach of

B. Scheme of mutagenesis for SFV-A3
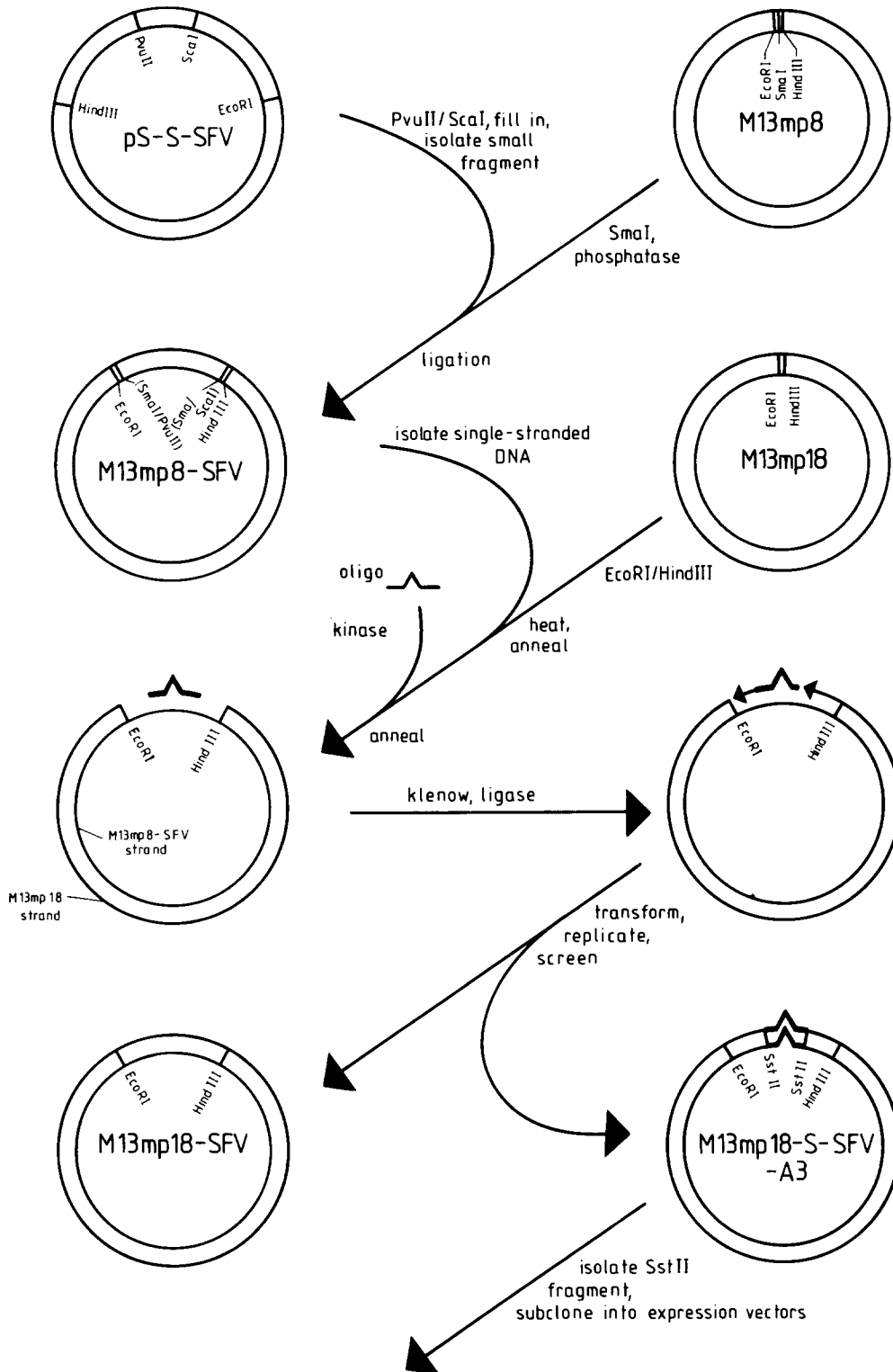
Dente et al. (10). The portion of a ssDNA phage (F1) required in *cis* for generation of ssDNA was cloned into the SV40-based expression vector pS-S-SFV (see Fig. 3*a*) to give pSFd (Fig. 2*a*). Superinfection of bacteria harboring this plasmid with a helper phage allows the isolation of sspSFd. The use of

pSFd allowed mutants to be rapidly tested by expression. The efficiency of mutagenesis with this system was ~0.5–1%.

For the creation of SFV-A3 (Fig. 2*b*), the initial target for hybridization of the oligonucleotide was limited to a 750-base pair Pvu II–Sca I segment by a gapped heteroduplex approach
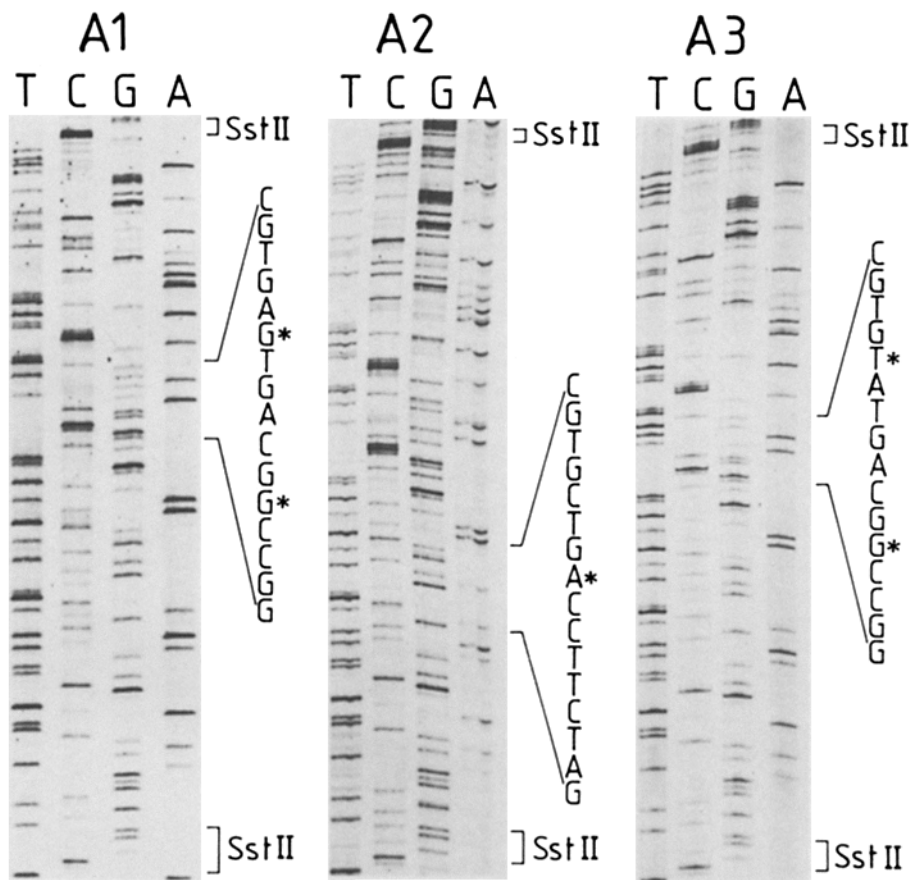
Figure 3. DNA sequence of the SFV-A mutations. The sequence of the three mutant 149-base pair SstII–SstII fragments used in these studies are shown. Lane headings indicate dideoxynucleotides used. The SstII recognition sequences are indicated as are the positions of incorporated mutagenic oligonucleotides. Starred bases in the oligonucleotides indicate changes from the wild-type sequence.

(28). The single-stranded template for SFV-A3 was produced by subcloning the 750-base pair fragment of the SFV cDNA into a plasmid based on an ssDNA phage, M13-mp8 (39), to produce M13-mp8-SFV. The use of the mp8/mp18 gapped duplex strategy allows genetic selection for the mutagenized daughter plasmids; by using the nonsuppressor host ES781 (6), the mp8-derived wild-type daughter plasmids are selected against since mp8 (unlike mp18) carries two amber mutations. ES781 has the additional advantage that it also lacks the MutL mismatch repair system and so will not convert the heteroduplex plasmids to homoduplexes, a process which normally favors the in vivo–methylated wild-type strand and therefore reduces the yield (29). The efficiency of mutagenesis in M13mp8-SFV was about 10-fold greater than with pSFd, 5–10%. All three mutants were isolated by hybridization screening (7) followed by restriction analysis and confirmed by sequencing using the dideoxy method between the two flanking SstII sites (Fig. 3). The SstII–SstII fragment was then subcloned into the expression vectors used in these studies ensuring that only the desired mutations were present in the proteins being analyzed.

Expression of p62/E2 with and without E1

The SstII–SstII fragments encoding the A-mutants were cloned into two different kinds of SFV expression plasmids; pS-S-SFV and pL1-SFV. The first (Fig. 4a) is based on the SV40 early region and has been described (27). The latter (Fig. 4b) is the SV40 late region expression vector of Gruss et al. (18) with the SFV-cDNA inserted (Melancon, P., unpublished data). The pS-S-SFV series of plasmids encoding wild-

type and mutant cDNAs were used for microinjection experiments. The pL1-SFV series were transfected into COS-7 cells where the endogenously expressed T-antigen promotes replication and transcription from the late region of SV40 DNA. This amplification facilitated experiments where the proteins produced were analyzed by electrophoresis. Since E1, which is co-expressed with p62 from SFV expression plasmids, may help to stabilize the latter in the membrane (in the p62-E1 spike complex) and therefore mask alterations in its phenotype, p62 has been expressed and analyzed both in the presence and the absence of E1 (see Fig. 5). To express p62 in the absence of E1, we have used the plasmid pL1-SFV-d9 where the SFV cDNA is truncated in the middle of the 6K-peptide region (up to the codon for Ala 24). This 60–amino acid residue peptide is found between p62 and E1 and is cleaved away co-translationally. The p62 protein produced from pL1-SFV-d9 will, most likely, undergo normal E2/6K cleavage and give rise to a p62 without the aberrant amino acids at its carboxyl terminus commonly introduced in truncations (e.g., 9, 15). The truncation SFV-d9 (Fig. 5) is one of a series described elsewhere (15) and has been subcloned into pA11-SVL2 to produce pL1-SFV-d9 (Fig. 4c and Materials and Methods).

Size and Glycosylation of the SFV-A Mutants

The first analysis of the SFV-A mutants was designed to show that the wild-type and mutant p62 proteins expressed from both pL1-SFV and pL1-SFV-d9 are the expected sizes, with and without oligosaccharides. Accordingly, two sets of all eight plasmids (wild-type and mutants, pL1-SFV and pL1-
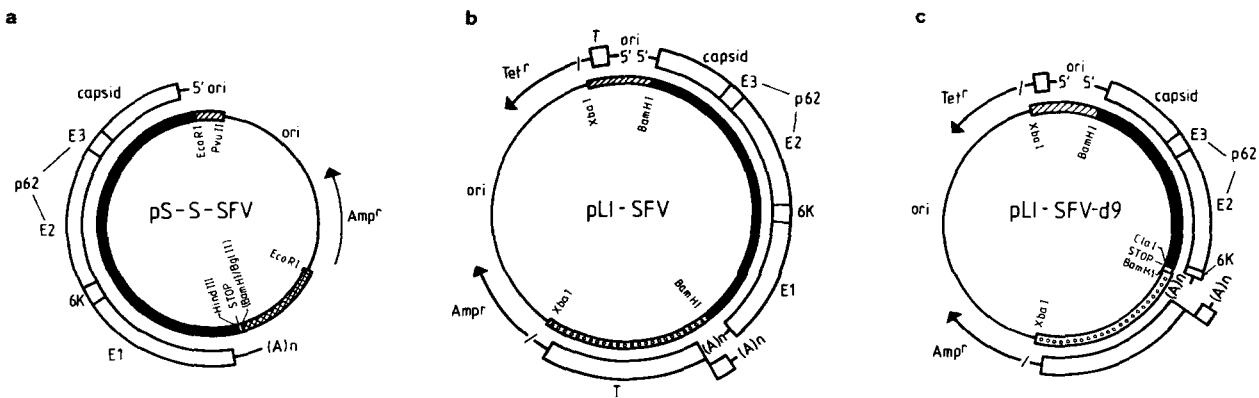
Figure 4. Expression vectors used in these experiments. Drawn to the same scale, these diagrams show both the functional units in the DNA (inner circles) and the predicted RNA transcripts (outer circles) with the regions coding for SFV proteins boxed. In the DNA, a solid thick line indicates SFV coding region. A hatched region includes the SV40 early promoter (pS-S-SFV) or the early and late promoters, origin of replication plus the beginning of the T-antigen gene (pL1-SFV and pL1-SFV-d9). The region with circles includes the rest of the T-antigen coding region and SV40 polyadenylation signals. Cross-hatching (pS-S-SFV) indicates polyadenylation signal for SV40.
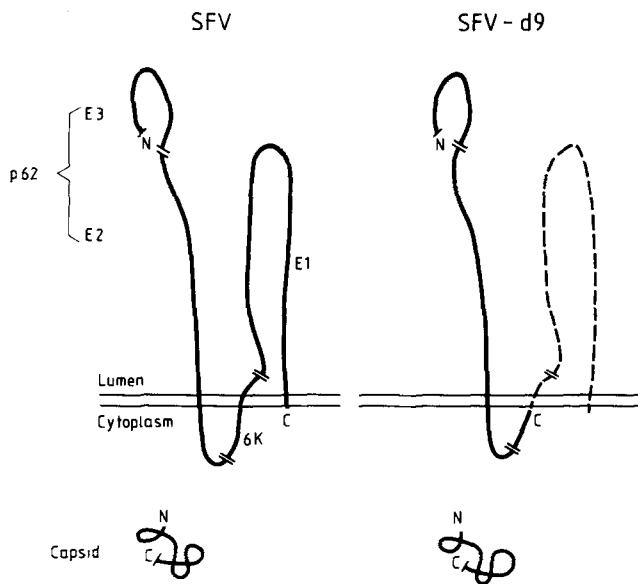
Figure 5. The SFV spike, and the SFV-d9 deletion. The proteins (capsid-E$_3$-E2-6K-E1) encoded by the full length SFV-cDNA and SFV-d9 (capsid-E$_3$-E2) are shown. The region deleted in d9 is shown as an interrupted line. The sites of proteolytic processing of the polyprotein precursor are shown by double perpendicular lines. The disposition of the 6K peptide in the membrane is hypothetical.

SFV-d9) were transfected into COS-7 cells using DEAE-dextran (Materials and Methods). 30 h after transfection, one set of dishes was treated with tunicamycin and both were then pulse labeled with [^{35}S]methionine followed by solubilization, immunoprecipitation, gel electrophoresis, and fluorography (Fig. 6). Lanes 2–9 show that in cells transfected with pL1-SFV (and therefore co-expressing E2 and E1), the A1 and A3 forms of p62s migrate with the wild-type p62 both in the presence (*a*) or the absence (*b*) of NH$_2$-linked sugars. The concentration of tunicamycin sufficient to completely prevent *N*-glycosylation also inhibits protein synthesis considerably (compare even and odd tracks). The A2 form of p62, on the other hand, consistently migrates a little slower on SDS polyacrylamide gels, a pattern maintained in the presence of tunicamycin. In cells transfected with pL1-SFV-d9 and there-

fore lacking E1 (tracks 10–17), p62 migrates as a doublet. The major, faster-migrating form of p62 co-migrates with p62 produced in the presence of E1. This is consistent with the expected E2/6K cleavage. The A-mutants are glycosylated as wild-type, A2 again migrating slower. The slower migrating p62 form seen in the absence of E1 is probably not the uncleaved p62-6K protein since the predicted difference in molecular weight resulting from this cleavage in SFV-d9 is too small to account for the difference in mobility. p62 often runs as multiple bands on SDS gels (see, for example, reference 15), possibly due to different conformations of this cysteine-rich protein. It may be that the absence of E1 exaggerates this tendency—more marked in the case of A2 (see lane 4 where a doublet occurs even in the presence of E1). An alternative possibility, that the upper band is an intermediate in posttranslational modification has been tested. A 4-h chase does not alter this banding pattern (Cutler, D., unpublished observations). However, the doublet is not always present in samples analyzed by Western blot 40 h after transfection (see, for example, Fig. 3 in the following paper), and therefore may result from some incomplete posttranslational modification. The aberrant mobility of A2-p62 may be due to altered SDS binding since a charge has been placed into the most hydrophobic portion of the molecule. Interestingly, the level of expression of p62 is approximately three- to fivefold better in the absence of E1. Shortening the SFV cDNA consistently produces higher levels of expression after DEAE–dextran transfection (Melancon, P., and D. Cutler, unpublished observations). Lane 1 shows the nonspecific bands immunoprecipitated in this experiment.

Cell Surface Transport of the SFV-A Mutants

One of the simplest ways to test whether or not the A-mutants are still membrane associated is to look for cell surface expression. If the proteins are on the cell surface then they are still membrane associated. Moreover, we can use cell surface transport as a screen against possible pleiotropic effects of mutagenesis since the cellular machinery will often fail to transport proteins with even relatively small alterations in primary structure (3). Unaltered cell surface transport would be evidence of a functionally unaltered protein. Accordingly,
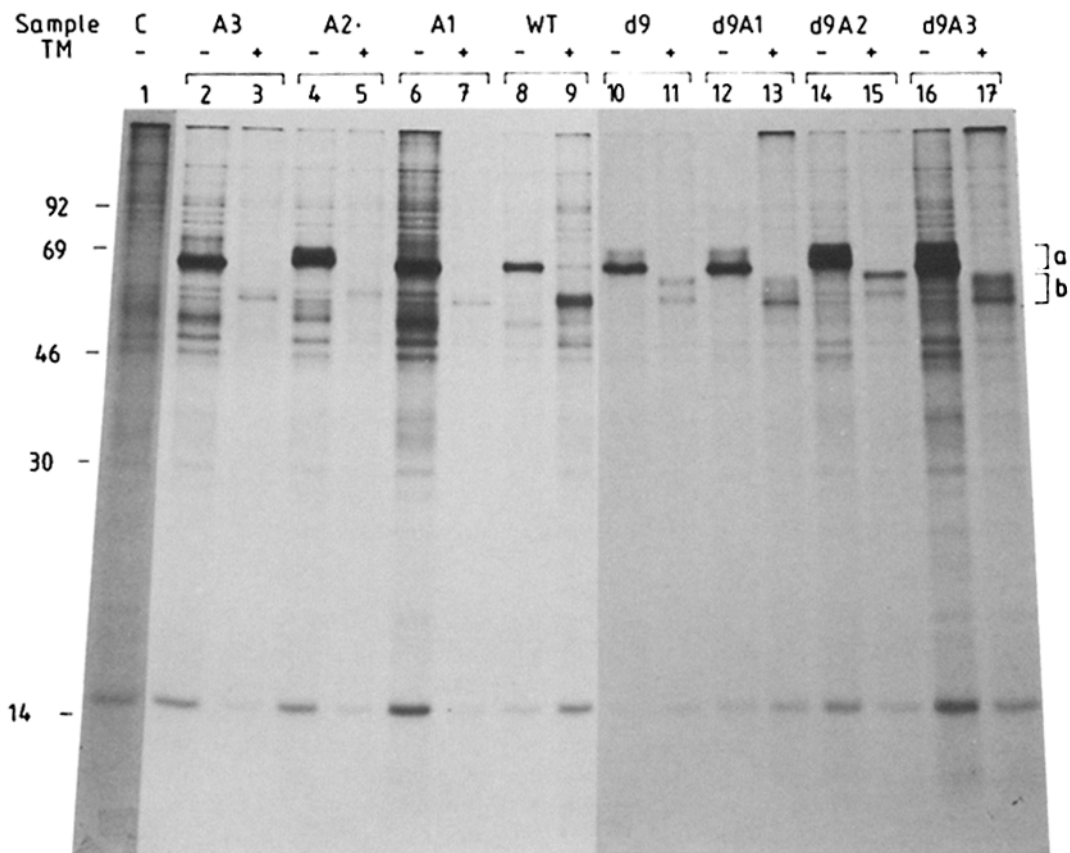
Figure 6. Size and glycosylation of the SFV-A mutants. 5-cm dishes of COS cells were transfected, labeled with or without tunicamycin treatment, and lysed. Lysates were immunoprecipitated with an anti-E2 IgG fraction, electrophoresed on a 10% gel, and the gel was fluorographed. The samples transfected (*WT, A3, A2, A1* refer to the wild-type and mutant spikes expressed from pL1-SFV; the *d9, d9A1, d9A2, d9A3* refer to the wild-type and mutant p62's expressed from pL1-SFV-d9) and the presence or absence of tunicamycin are indicated. *C* indicates untransfected cells. The migration of marker proteins (in kD) is indicated. *a* and *b* refer to p62 produced in the absence or presence of tunicamycin, respectively. The product of half of one dish (~1 × 10⁶ cells) of cells was loaded onto each track. Lanes 2–9 were from a 4-d exposure to an insensitive X-ray film, and lanes 1, and 10–17 from an overnight exposure to a sensitive film, all from one gel.

the pS-S-SFV versions of the wild-type and mutant SFVs were microinjected into BHK-21 cells and distribution was analyzed by surface and internal indirect immunofluorescence. Fig. 7, *a* and *b*, shows that all three mutants are capable of reaching the cell surface. The internal staining (Fig. 7, *c–e*) of cells microinjected with both wild-type and mutant cDNAs shows a reticular pattern with a perinuclear concentration and clearly visible cellular margins, typical for a normal plasma membrane protein. This fluorescent analysis has been repeated in COS-7 cells, following expression from the pL1-SFV series after DEAE–dextran transfection. The results obtained are similar to those seen with BHK-21 cells (Cutler, D., unpublished observations).

Can the A-mutant p62 proteins reach the cell surface in the absence of E1? Transfection of COS-7 cells with the four pL1-SFV-d9 plasmids followed by surface and internal indirect immunofluorescence (Fig. 8) shows that E1 is not required for surface appearance of the wild-type and the A-mutants of p62.

A fluorescent analysis of surface transport has limitations. It will not reveal small differences between wild-type and mutant p62s and cannot be used to rule out the possibility that only a subpopulation of the protein is reaching the cell surface. To pursue these latter points, the posttranslational processing of p62 into E3 + E2 has been exploited to achieve

an indirect measure of cell surface appearance. This cleavage is taking place either on the cell surface and/or just before the p62 proteins arrive to the cell surface; E2 is not found within the cell but only on its surface and in budded virions during infection (48). Transfection experiments reported earlier (15, 27) and in the accompanying paper (see in particular Fig. 3 of that report) have shown that efficient cleavage can only be obtained when the p62 protein is co-expressed with the E1 glycoprotein. Presumably, the E1-p62 interaction in the SFV spike glycoprotein supports a conformation recognized by the endoprotease. Furthermore, it is evident from Fig. 6 in this paper that long incubation times are needed to process the p62 protein in pL1-SFV DNA-transfected COS cells. After a 1-h pulse (without chase) of transfected cells, there is still very little E2 protein appearing both for wild-type and mutants (see faint band co-migrating with a nonspecific one in the 50-kD region in lanes 2–9 of Fig. 6). For these reasons, the ratio of total p62 to E2 has been measured in cells 40 h after transfection, in the presence of E1, using the pL1-SFV wild-type and mutant DNAs. After solubilization, samples were electrophoresed and transferred to nitrocellulose and stained with anti-E2 antibody followed by ¹²⁵I–protein A. Autoradiographs were scanned for quantitation. The results of three experiments (Table I) show E2/p62 ratios of about 2 both for
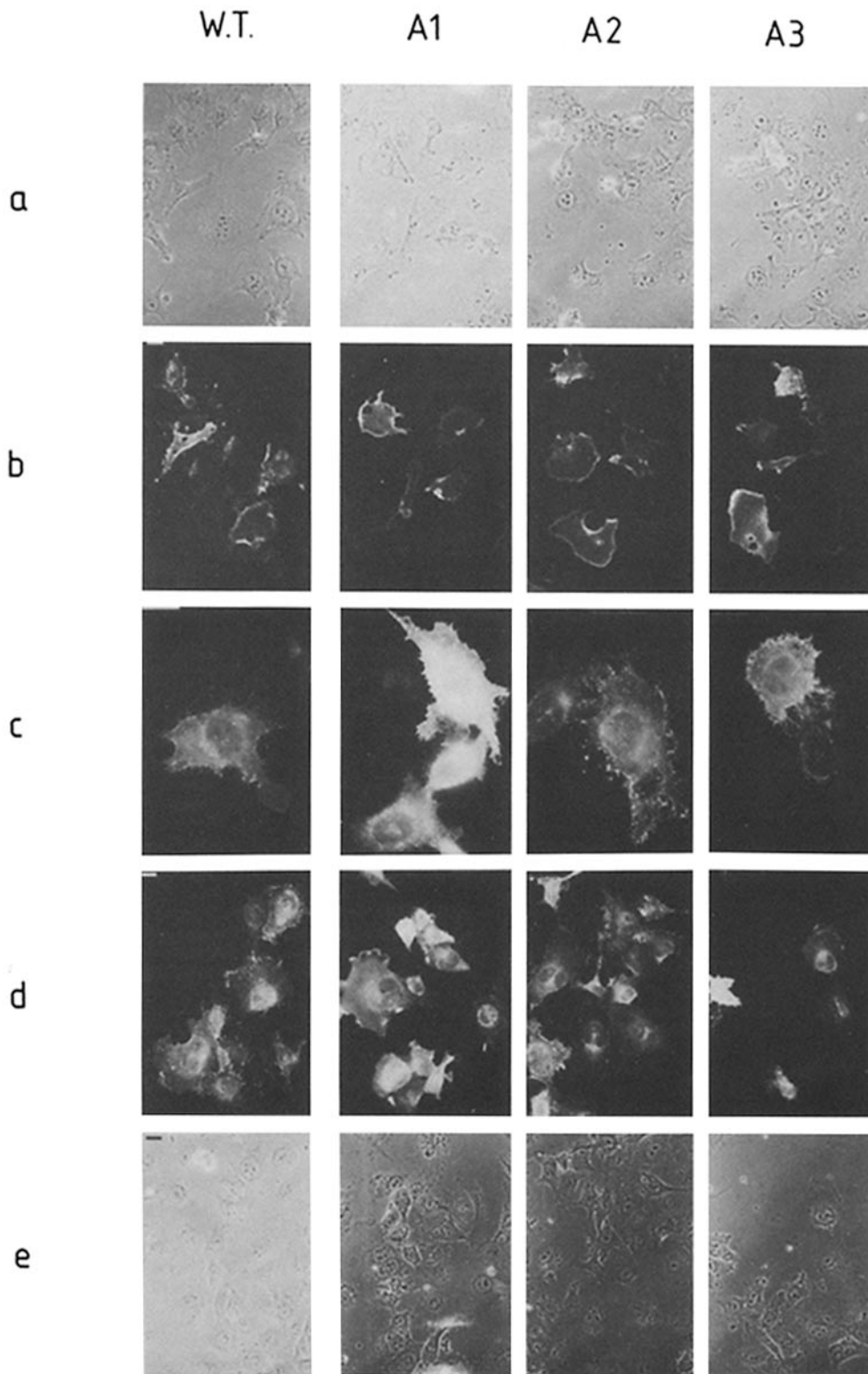
Figure 7. Surface and internal fluorescence of BHK-21 cells microinjected to produce wild-type and mutant SFV spikes. Nuclei of BHK-21 cells were microinjected with the pS-S-SFV constructs, fixed 6 h later, and stained with anti-E2 antibody or first permeabilized and then stained. Rows *a* and *b* show immunofluorescence and corresponding phase-contrast images of nonpermeabilized cells. Rows *d* and *e* show immunofluorescence and corresponding phase-contrast images of permeabilized cells. Row *c* shows cells treated as in *d* but at a 2.5-fold greater magnification. Bars, 20 μm.

the wild-type protein and all of the mutants. We conclude that all p62 mutants are transported to the cell surface with an efficiency similar to that of wild-type p62 protein.

Fusogenic Activity of the SFV-A Mutants

A function of the SFV spike complex that is directly related to its membrane binding is its activity as a fusogen. For the spike to promote fusion it must be anchored in a lipid bilayer

(36). It might be that fusion activity would be a very sensitive assay for functionally intact membrane binding. BHK-21 cells were microinjected with the four pSV-S-SFV plasmids containing the wild-type and A-mutant SFVs, left for 6 h, then briefly treated with low pH. After fixation, the cells were stained with anti-E2 antibody and photographed. Fig. 9 shows that all three mutant spikes, like the wild-type spike, exhibit fusogenic activity. In all cases, the microinjected cells express-
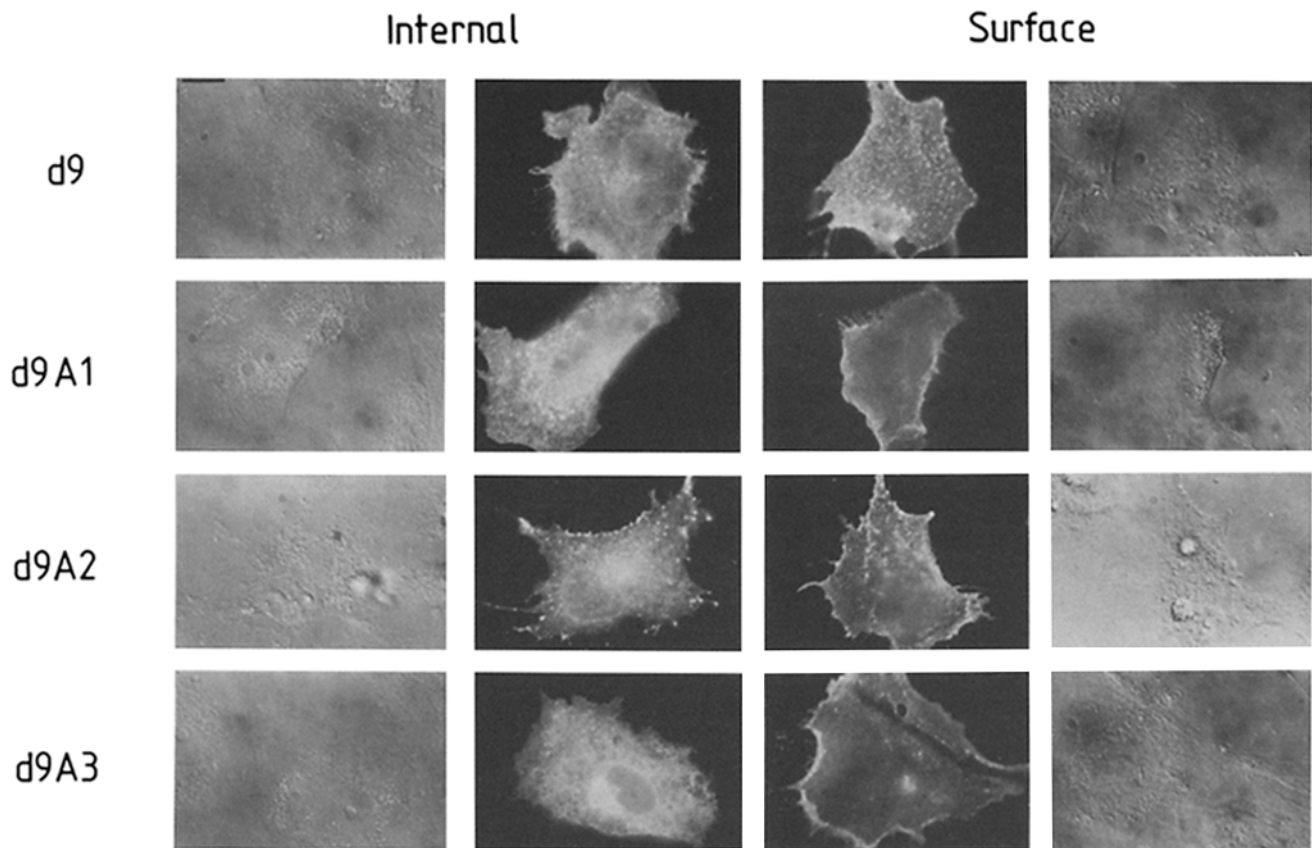
Internal   Surface

d9

d9 A1

d9A2

d9A3

Figure 8. Surface and internal fluorescence of COS-7 cells transfected to produce wild-type and mutant p62 proteins. COS-7 cells were transfected with the pL1-SFV-d9 constructs, left 40 h, fixed, and then stained with an anti-E2 antibody (*right-hand columns*) or permeabilized and then stained (*left-hand columns*). Fluorescent and corresponding Nomarski micrographs are shown. Bar, 20 μm.

ing wild-type or mutant spikes become a part of large polykaryons.

Discussion

In this paper the generation of three mutants of the membrane-binding polypeptide region of SFV-p62/E2 is described. After expression, the mutated DNAs express proteins of the predicted size. These are glycosylated and transported to the cell surface as is the wild-type p62/E2, both in the presence and absence of E1. Moreover, all three spikes made with mutated p62/E2 display fusogenic activity.

The demonstration of normal cell surface appearance and fusogenic activity for the SFV-A mutants rules out the possibility that the mutations have completely destroyed the functioning of the membrane-binding region of the p62/E2 polypeptide. Moreover, cell surface appearance is an important feature of our mutants since we wanted to make only those minimal alterations to p62/E2 structure that are consistent with alterations to its membrane-binding polypeptide region. The field of mutagenesis/expression shows many examples where engineering at the DNA level has led to impaired intracellular transport (e.g., references 12, 19, 38, and 46). These results are often very difficult to interpret and so we have attempted to produce proteins that are as little perturbed as possible; efficient cell surface transport argues that we have achieved this.

Our results with A2 are in contrast with those recently published by Adams and Rose (1). They show that the sub-

Table I. Ratio of E2 to p62 in Cells Transfected with pL1-SFV Encoding Wild-type and Mutant E2/p62 Proteins

Sample	Wild type	A1	A2	A3
E2/p62*	2.1 ± 0.14	1.8 ± 0.28	1.9 ± 0.74	1.7 ± 0.2

Cells transfected with indicated DNAs were solubilized after 40 h. Samples were Western blotted and stained with anti-E2 antibody followed by ^{125}I-protein A. Autoradiographs were scanned, peaks cut out, and weighed. Data presented is the mean of three experiments ± SEM.
* The weight of the E2 peak/the weight of the p62 peak.

stitution of an Arg for an Ile in the middle of the hydrophobic stretch of VSV-G seriously inhibits its surface transport. There are at least two possible reasons for this difference in result. If the interaction between lipid bilayer and hydrophobic spanning stretch is important for intracellular transport then disrupting this interaction could inhibit that transport. Arg could well be more disruptive than Glu (31). Moreover, while the membrane-spanning stretch of VSV-G is defined by a charge at both ends, that of p62/E2 does not have a charge-defined NH2-terminal border (see Fig. 1). Thus p62/E2 may be able to slide upstream in the mechanism, thereby avoiding the problem of burying a charge in the bilayer. A second possibility is that oligomerization of VSV-G is important for its cell surface transport and that the mutation affects this. In the case of SFV, the spike of which is a hetero-oligomer (unlike the glycoprotein of VSV), it could be either that Glu does not affect oligomerization or that the transport of p62 is not very sensitive to its oligomeric state. This may well be so
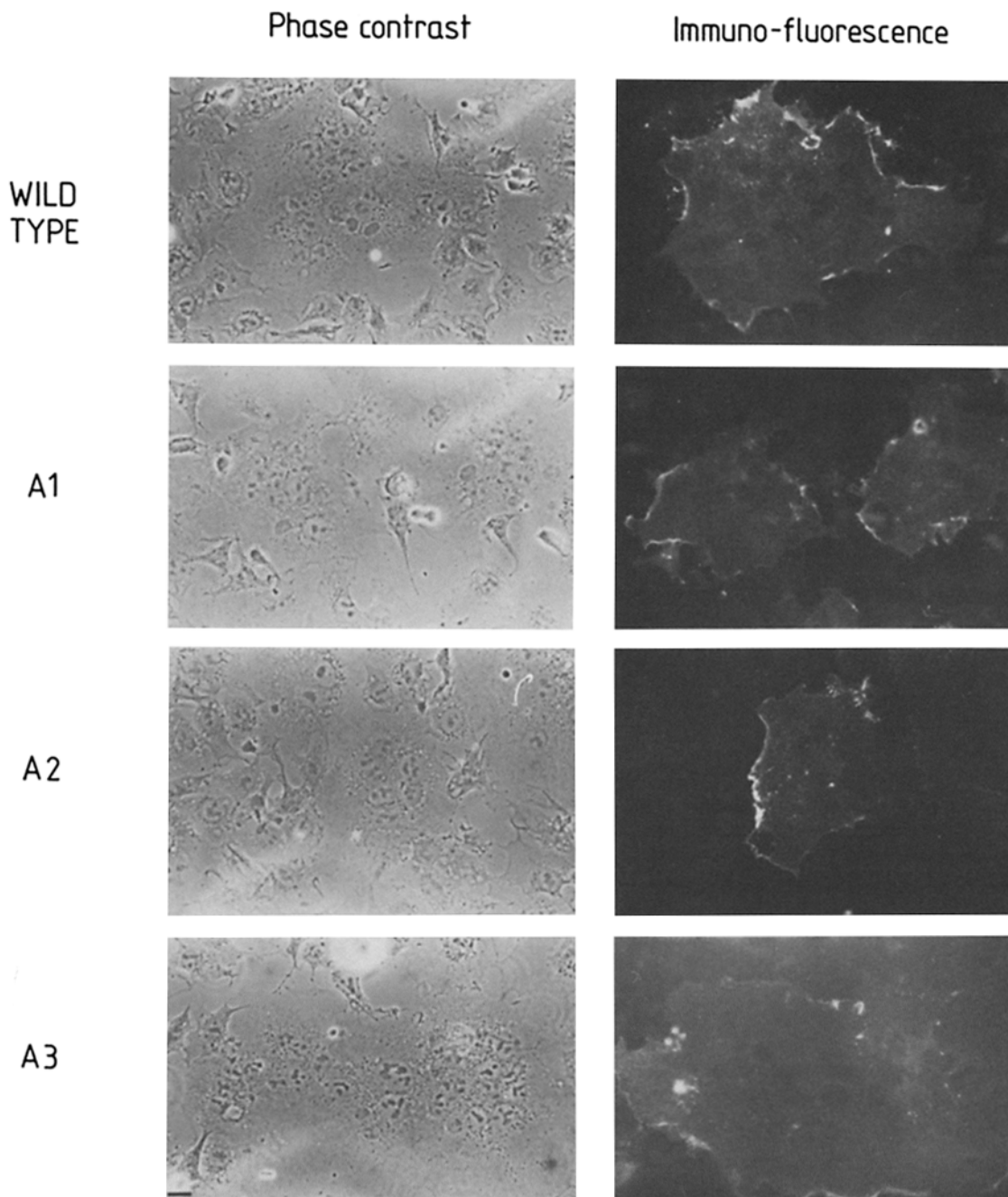
Figure 9. Fusion activity of wild-type and SFV-A mutant spikes. BHK-21 cells were microinjected with the pS-S-SFV constructs, left for 6 h, then briefly washed with medium at pH 5.5 and left for 1 h. They were then fixed and stained with anti-E2 antibody. Immunofluorescence and the corresponding phase-contrast images are shown. Bar, 20 μm.

since p62 can reach the cell surface in the absence of E1.

We have argued that since membrane binding of spike proteins is essential for fusion (36) and all three mutants of p62/E2 cause cell–cell fusion, all three SFV-A-mutants have unaltered membrane binding. However, the fusion activity of the SFV spike has only been found when the whole complex is expressed; p62 expressed alone cannot cause fusion (27). This result implies that SFV-E1 may have a primary role in fusion. However, when expressed alone, E1, although glycosylated and therefore translocated, does not reach the cell surface (22, and Melancon, P., unpublished data) and therefore we have no positive confirmation of a primary fusogenic

role for E1 in SFV. Thus, it may be that both E1 and E2 are required in concert to mediate fusion (52). That our mutations do not appear to affect fusion may therefore reflect either that p62/E2 is not involved in fusion or that they do not impair functional membrane binding of p62/E2.

Both assays of membrane association presented here are functional and therefore indirect. It could be that the position and/or stability of the mutant proteins in the membrane is altered in these mutants despite their unimpaired functioning. In the following paper, we directly address these questions.

The general implication of the results presented here is that it is unlikely that a specific structure present in the membrane-

binding polypeptide region is being recognized by some machinery involved in translocation leading to the halting of transfer. Our data tend to support a model in which a general hydrophobicity causes a transmembrane protein to assume its three-domain structure, and that an intact charge cluster and uninterrupted hydrophobic stretch are not important for this function.

References

1. Adams, G. A., and J. K. Rose. 1985. Incorporation of a charged amino acid into the membrane-spanning domain blocks cell surface transport but not membrane anchoring of a viral glycoprotein. *Mol. Cell Biol.* 5:1442–1448.

2. Alt, F. W., A. L. M. Bothwell, M. Knapp, E. Siden, E. Mather, M. Koshland, and D. Baltimore. 1980. Synthesis of secreted and membrane-bound immunoglobulin β heavy chains is directed by mRNAs that differ at their 3′ ends. *Cell.* 20:293–301.

3. Arias, C., J. R. Bell, E. M. Lenches, E. G. Strauss, and J. H. Strauss. 1983. Sequence analysis of two mutants of Sindbis virus defective in the intracellular transport of their glycoproteins. *J. Mol. Biol.* 168:87–102.

4. Blobel, G. 1978. Mechanisms for the intracellular compartmentation of newly synthesised proteins. *Proc. 11th FEBS Meeting.* BFC Clark, editor. Oxford: Pergamon.

5. Boeke, J. D., and P. Model. 1982. A prokaryotic membrane anchor sequence: carboxyl terminus of bacteriophage F1 gene III protein retains it in the membrane. *Proc. Natl. Acad. Sci. USA.* 79:5200–5204.

6. Caillet-Fauquet, P., G. Maenhaut-Michel, and M. Radman. 1984. SOS mutator effect in *E. coli* mutants deficient in mismatch repair. *EMBO (Eur. Mol. Biol. Organ.) J.* 3:707–712.

7. Carter, P. J., G. Winter, A. J. Wilkinson, and A. R. Fersht. 1984. The use of double mutants to detect structural changes in the active site of the Tyrosyl-tRNA synthetase (*Bacillus stearothermophillus*). *Cell.* 38:835–840.

8. Compans, R. W., H. D. Klenk, L. A. Caliguiri, and P. W. Choppin. 1970. Influenza virus proteins. I. Analysis of polypeptides of the virion and identification of spike glycoproteins. *Virology.* 42:880–889.

9. Davis, N. G., J. D. Boeke, and P. Model. 1985. Fine structure of a membrane anchor domain. *J. Mol. Biol.* 181:111–121.

10. Dente, L., G. Cesarini, and R. Cortese. 1983. pEMBL: a new family of single stranded plasmids. *Nucleic Acids Res.* 11:1645–1655.

11. Dotto, G. P., and K. Horiuchi. 1981. Replication of a plasmid containing two origins of bacteriophage F1. *J. Mol. Biol.* 153:169–176.

12. Doyle, C., M. G. Roth, J. S. Sambrook, and M.-J. Gething. 1985. Mutations in the cytoplasmic domain of the influenza virus hemagglutinin affect different stages of intracellular transport. *J. Cell. Biol.* 100:704–714.

13. Garoff, H., and H. Söderlund. 1978. The amphiphillic membrane glycoproteins of Semliki Forest virus are attached to the lipid bilayer by their COOH-terminal ends. *J. Mol. Biol.* 124:535–549.

14. Garoff, H., A.-M. Frischauf, K. Simons, H. Lehrach, and H. Delius. 1980. Nucleotide sequence of cDNA coding for Semliki Forest virus membrane glycoprotein. *Nature (Lond.).* 288:236–241.

15. Garoff, H., C. Kondor-Koch, R. Pettersson, and B. Burke. 1983. Expression of Semliki Forest virus proteins from cloned complementary DNA. II. The membrane-spanning glycoprotein E2 is transported to the cell surface without its normal cytoplasmic domain. *J. Cell Biol.* 97:652–658.

16. Garoff, H. 1985. Using recombinant DNA techniques to study protein targeting in the eucaryotic cell. *Ann. Rev. Cell Biol.* 1:403–445.

17. Gething, M.-J., and J. Sambrook. 1982. Construction of influenza hemagglutinin genes that code for intracellular and secreted forms of the protein. *Nature (Lond.)* 300:598–603.

18. Gruss, P., N. Rosenthal, M. Konig, R. W. Ellis, T. Y. Shih, E. M. Scholnick, and G. Khoury. 1982. The expression of viral and cellular p21 *ras* genes using SV40 as a vector. *In* Eukaryotic Viral Vectors. J. Gluzman, editor. Cold Spring Harbor Laboratory. 13–19.

19. Guan, J.-L., and J. K. Rose. 1984. Conversion of a secretory protein into a transmembrane protein results in its transport to the Golgi complex but not to the cell surface. *Cell.* 37:779–787.

20. Guild, B. C., and J. L. Strominger. 1984. Human and murine class I MHC antigens share conserved serine 335, the site of HLA phosphorylation in vivo. *J. Biol. Chem.* 259:9235–9240.

21. Hanahan, D. 1983. Studies on transformation of *E. coli* with plasmids. *J. Mol. Biol.* 166:557–580.

22. Hashimoto, K., S. Erdel, S. Keränen, J. Saraste, and L. Kääriäinen. 1981. Evidence for a separate signal for the carboxy-terminal envelope glycoprotein E1 of Semliki Forest virus. *J. Virol.* 38:34–40.

23. Henning, R., R. J. Milner, K. Reske, B. A. Cunningham, and G. M. Edelman. 1976. Subunit structure, cell surface orientation, and partial amino acid sequences of murine histocompatibility antigens. *Proc. Natl. Acad. Sci. USA.* 73:118–122.

24. Holland, T. C., F. L. Homa, S. D. Marlin, M. Levine, and J. Glioroso. 1984. Herpes Simplex virus type 1 glycoprotein C-negative mutants exhibit multiple phenotypes, including secretion of truncated glycoproteins. *J. Virol.* 52:566–574.

25. Hortsch, M., and D. I. Meyer. 1984. Pushing the signal hypothesis: what are the limits? *Biol. Cell.* 52:1–8.

26. Katz, F. N., J. E. Rothman, V. R. Lingappa, G. Blobel, and H. F. Lodish. 1977. Membrane assembly in vitro: synthesis, glycosylation, and asymmetric insertion of a transmembrane protein. *Proc. Natl. Acad. Sci. USA.* 74:3278–3282.

27. Kondor-Koch, C., B. Burke, and H. Garoff. 1983. Expression of Semliki Forest virus proteins from cloned complementary DNA. I. The fusion activity of the spike glycoprotein. *J. Cell Biol.* 97:644–651.

28. Kramer, J., V. Drutsa, H.-W. Jansen, B. Kramer, M. Pfugfelder, and H.-J. Fritz. 1984. The gapped duplex approach to oligonucleotide-directed mutation construction. *Nucleic Acids Res.* 12:9441–9456.

29. Kramer, W., K. Schughart, and H.-J. Fritz. 1982. Directed mutagenesis of DNA cloned in filamentous phages: influence of hemimethylated DNA GATC sites on marker recovery from restriction fragments. *Nucleic Acids Res.* 10:6475–6485.

30. Kress, M., D. Cosman, G. Khoury, and G. Jay. 1983. Secretion of a transplantation-related antigen. *Cell.* 34:189–196.

31. Kyte, J., and R. F. Doolittle. 1982. A simple method for displaying the hydropathic character of a protein. *J. Mol. Biol.* 157:105–132.

32. Lehrman, M. A., W. J. Schneider, T. C. Südhof, M. S. Brown, J. L. Goldstein, and D. W. Russell. 1985. Mutation in LDL receptor: Alu-Alu recombination deletes exons encoding transmembrane and cytoplasmic domains. *Science (Wash. DC).* 227:140–146.

33. Lingappa, V. R., F. N. Katz, H. F. Lodish, and G. Blobel. 1978. A signal sequence for the insertion of a transmembrane glycoprotein. *J. Biol. Chem.* 253:8667–8670.

34. Liscum, L., J. Finer-Moore, R. M. Stroud, K. L. Luskey, M. S. Brown, and J. L. Goldstein. 1985. Domain structure of 3-hydroxy-3-methylglutaryl coenzyme A reductase, a glycoprotein of the endoplasmic reticulum. *J. Biol. Chem.* 260:522–530.

35. Maniatis, T. E., E. F. Fritsch, and J. Sambrook. 1982. Molecular cloning: a laboratory manual. Cold Spring Harbor Laboratory. New York.

36. Marsh, M., E. Bolzau, J. White, and A. Helenius. 1983. Interaction of Semliki spike glycoprotein rosettes and vesicles with cultured cells. *J. Cell Biol.* 96:455–461.

37. Matlin, K. S., and K. Simons. 1984. Sorting of an apical plasma membrane glycoprotein occurs before it reaches the cell surface in cultured epithelial cells. *J. Cell Biol.* 99:2131–2139.

38. McQueen, N. L., D. P. Nayak, L. V. Jones, and R. W. Compans. 1984. Chimeric influenza virus hemagglutinin containing either the NH_2 terminus or the COOH terminus of G protein of vesicular stomatitis virus is defective in transport to the cell surface. *Proc. Natl. Acad. Sci. USA.* 81:395–399.

39. Messing, J. 1983. New M13 vectors for cloning. *Methods Enzymol.* 101:20–78.

40. Messing, J., B. Gronenborn, R. Müller-Hill, and P. H. Hofschneider. 1977. Filamentous coliphage M13 as a cloning vehicle: Insertion of a Hind III fragment of the *lac* regulatory region in M13 replicative form *in vitro. Proc. Natl. Acad. Sci. USA.* 74:3642–3646.

41. Pettersson, R. F., K. Lunström, J. B. Chattopadhyaya, S. Josephson, L. Philipson, L. Kääriäinen, and I. Palva. 1983. Chemical synthesis and molecular cloning of a STOP oligonucleotide encoding for an UGA translation terminator in all three reading frames. *Gene.* 24:15–27.

42. Rice, C. M., J. R. Bell, M. W. Hunkapiller, E. G. Straus, and J. H. Straus. 1982. Isolation and characterization of the hydrophobic COOH-terminal domains of the Sindbis virion glycoproteins. *J. Mol. Biol.* 154:355–378.

43. Riedel, H. 1985. Different membrane anchors allow the Semliki Forest virus spike subunit E2 to reach the cell surface. *J. Virol.* 54:224–228.

44. Rogers, J., P. Early, C. Carter, K. Calame, M. Bond, L. Hood, and R. Wall. 1980. Two mRNAs with different 3′ ends encode membrane-bound and secreted forms of immunoglobulin β chain. *Cell.* 20:303–312.

45. Rose, J. K., and J. E. Bergman. 1982. Expression from cloned cDNA of cell-surface secreted forms of the glycoprotein of vesicular stomatitis virus in eukaryotic cells. *Cell.* 30:753–762.

46. Rose, J. K., and J. E. Bergman. 1983. Altered cytoplasmic domains affect intracellular transport of the vesicular stomatitis virus glycoprotein. *Cell.* 34:513–524.

47. Sabatini, D. D., G. Kreibich, T. Morimoto, and M. Adesnik. 1982. Mechanisms for the incorporation of proteins in membranes and organelles. *J.*

Cell Biol. 92:1–22.

48. Simons, K., and G. Warren. 1984. Semliki Forest virus: a probe for membrane traffic in the animal cell. *Adv. Protein Chem.* 36:79–132.

49. Thomas, M. L., A. N. Barclay, J. Gagnon, and A. F. Williams. 1985. Evidence from cDNA clones that the rat leucocyte common antigen (T200) spans the lipid bilayer and contains a cytoplasmic domain of 80,000 M_r. *Cell.* 41:83–93.

50. Timm, B., C. Kondor-Koch, H. Lehrach, H. Riedel, J.-E. Edström, and H. Garoff. 1983. Expression of viral membrane proteins from cloned cDNA by microinjection into eukaryotic cell nuclei. *Methods Enzymol.* 96:496–511.

51. Warren, G. 1981. Membrane proteins: structure and assembly. *In* Membrane Structure. J. B. Finean and R. H. Michell, editors. Elsevier/North Holland, Amsterdam. 215–257.

52. White, J., M. Kielian, and A. Helenius. 1983. Membrane fusion proteins of enveloped animal viruses. *Q. Rev. Biophys.* 16:151–195.

53. Wills, J. W., R. V. Srinavas, and E. Hunter. 1984. Mutations of the Rous Sarcoma virus *env* gene that affect the transport and subcellular location of the glycoprotein products. *J. Cell Biol.* 99:2011–2023.

54. Yost, C. S., J. Hedgpeth, and V. R. Lingappa. 1983. A stop transfer sequence confers predictable transmembrane orientation to a previously secreted protein in cell-free systems. *Cell.* 34:759–766.

55. Zoller, M. F., and M. Smith. 1983. Oligonucleotide-directed mutagenesis of DNA fragments cloned into M13 vectors. *Methods Enzymol.* 100:468–500.

56. Zuniga, M. C., B. Malissen, M. McMillan, P. R. Brayton, S. S. Clark, J. Forman, and L. Hood. 1983. Expression and function of transplantation antigens with altered or deleted cytoplasmic domains. *Cell.* 34:535–544.